07 - 10 September 2009

PROCEEDINGS

54. IWK

Internationales Wissenschaftliches Kolloquium
International Scientific Colloquium

Information Technology and Electrical Engineering - Devices and Systems, Materials and Technologies for the Future

Faculty of Electrical Engineering and Information Technology

Startseite / Index:
http://www.db-thueringen.de/servlets/DocumentServlet?id=14089

TECHNISCHE UNIVERSITÄT
ILMENAU

Impressum

Herausgeber: Der Rektor der Technischen Universität Ilmenau
Univ.-Prof. Dr. rer. nat. habil. Dr. h. c. Prof. h. c.
Peter Scharff

Redaktion: Referat Marketing
Andrea Schneider

Fakultät für Elektrotechnik und Informationstechnik
Univ.-Prof. Dr.-Ing. Frank Berger

Redaktionsschluss: 17. August 2009

Technische Realisierung (USB-Flash-Ausgabe):
Institut für Medientechnik an der TU Ilmenau
Dipl.-Ing. Christian Weigel
Dipl.-Ing. Helge Drumm

Technische Realisierung (Online-Ausgabe):
Universitätsbibliothek Ilmenau
ilmedia
Postfach 10 05 65
98684 Ilmenau

Verlag:
Verlag ISLE, Betriebsstätte des ISLE e.V.
Werner-von-Siemens-Str. 16
98693 Ilmenau

ISBN (USB-Flash-Ausgabe): 978-3-938843-45-1
ISBN (Druckausgabe der Kurzfassungen): 978-3-938843-44-4

Startseite / Index:
http://www.db-thueringen.de/servlets/DocumentServlet?id=14089

DESIGN OF CLOSED-LOOP CONTROLLERS FOR ELECTROMAGNETIC BEARINGS

Dipl. Ing.(FH) Ringo Lehmann, Prof. Dr. Ing. Lutz Zacharias

EAAT GmbH Chemnitz, Westsächsische Hochschule Zwickau; GERMANY

ABSTRACT

For many applications it is important to use magnetic bearings. The paper begins by expounding briefly the existing designs and fields of application for electromagnetic bearings. The levitation of the rotor within the stator is achieved by way of closed-loop control. This paper presents electromagnetic and magneto mechanical laws as the basis for detailed systematic and mathematical modeling of the control loop. The derived system describes the characteristic, inherently instable system behaviour. A cascaded controller structure is applied to achieve the desired control dynamics. Especially the master position controller will be parameterized using the root-locus method. Computer-aided optimization of the controller parameters utilizes simulation and provides reliable forecasts of the control loop behaviour. Furthermore the analogue control algorithm is discretised for implementation on a microprocessor based target hardware.

1. DIFFERENCES BETWEEN CONVENTIONAL AND MAGNETIC BEARINGS

Conventional roller) bearings consist of two combined movable components. Between these components there are solid rolling figures (rollers, balls). Lubricants reduce friction between these mechanical components. Mechanical influences affect all movable parts. In magnetic bearings the rolling figures will be replaced by magnetic forces so, that there aren't any moving solid parts inbetween.. Consequential there are following advantages:

- no soiling caused by wear
- no lubricants
- few vibration transfer between the rotor and stator
- available to use under extremely requirements (vacuum, clean-room, very high speeds)

But there are some disadvantages too:

- system needs additional electrical energy
- difficult construction

1.1. Construction of electromagnetic bearings

There are different types of magnetic bearings for technical application. These types are called homopolar, heteropolar and unipolar. Additionally these types are divided in radial, axial and permanent magnetic bearings. The structure determines the behaviour of the magnetic field in stator and rotor as well as size and magnetic losses. There is no explicit relation between construction and kind of closed-loop controller [1].

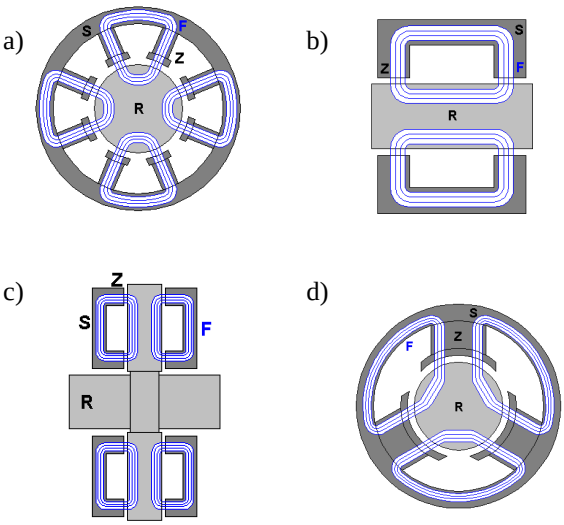

a) heteropolar electromagnetic bearing
b) homopolar electromagnetic bearing
c) axial electromagnetic bearing
d) unipolar electromagnetic bearing

(S=stator, R=rotor, Z=direction, F=flux lines of electromagnetic field)

Figure 1 Kinds of electromagnetic bearings

2. CONTROLLED SYSTEM

To design the closed-loop controller a first step is the mathematic derivation of the controlled system. No real component is absolutely linear, so it is necessary to use the behaviour of a linearised model instead. This mostly allows an easier handling of the system. That's why it is worth considering certain approaches of model downsizing, adaptation and order reduction.

So the symmetric structure of the electromagnetic bearing allows a simplified description as a mass-spring system. A current

converter serves as power supply for the bearing coil. The current through the coils initiates an according electromagnetic force. A position sensor detects the position difference between stator and rotor. Furthermore it is necessary to find a mathematical coherence between current, force and air gap.

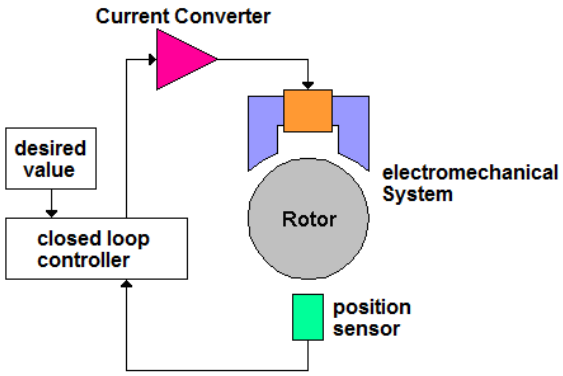

Figure 2 Schematic of closed loop controlled system

2.1. Electromechanical system part

It can be described using the equation set below:

$$\oint H \cdot dl = \Theta = l_{Fe} \cdot H_{Fe} + 2 \cdot \delta \cdot H_{air} \quad (2.1)$$

$$N \cdot i = l_{Fe} \cdot \frac{B}{\mu_{rFe} \cdot \mu_0} + 2 \cdot \delta \cdot \frac{B}{\mu_0} \quad (2.2)$$

$$\text{because } \mu_{rFe} >> 1 \rightarrow \lim_{\mu_{rFe} \to \infty} = \frac{l_{Fe}}{\infty} = 0 \quad (2.3)$$

$$B = \mu_0 \cdot \frac{N \cdot i}{2 \cdot \delta} \quad (2.4)$$

$$F = \frac{1}{\mu_0} \cdot \left(\frac{\mu_0 \cdot N \cdot i}{2 \cdot \delta} \right)^2 \cdot A_{Luft} = \frac{\mu_0 \cdot N^2 \cdot A_{Luft}}{4} \cdot \frac{i^2}{\delta^2} \quad (2.5)$$

$$k = \frac{\mu_0 \cdot N^2 \cdot A_{Luft}}{4}$$

$$\boxed{F = k \cdot \frac{i^2}{\delta^2}} \quad (2.6)$$

This is the general quadratic function between current and air gap.
Because of (2.6) a linearization is necessary.

$$F(i,\delta) = F(i_0,\delta_0) + \frac{\partial F(i,\delta)}{\partial i} \cdot \Delta i + \frac{\partial F(i,\delta)}{\partial \delta} \cdot \Delta \delta$$

$$F(i,\delta) = k \cdot \frac{{i_0}^2}{{\delta_0}^2} + \frac{2 \cdot i_0 \cdot k}{{\delta_0}^2} \cdot \Delta i + \frac{-2 \cdot {i_0}^2 \cdot k}{{\delta_0}^3} \cdot \Delta \delta \quad (2.7)$$

With $k_s = \frac{-2 \cdot {i_0}^2 \cdot k}{{\delta_0}^3}$ and $k_i = k \cdot \frac{{i_0}^2}{{\delta_0}^2} + \frac{2 \cdot i_0 \cdot k}{{\delta_0}^2}$ the electromechanical gain-coefficient is:

$$\boxed{K_{MF} = \frac{k_i}{k_s}} \quad (2.8)$$

The mechanical system is a mass-spring system.
$F = -D \cdot s \rightarrow m \cdot \ddot{s} = -D \cdot s \rightarrow \ddot{s} = -\omega^2 \cdot s \rightarrow -\omega^2 \cdot s \cdot m = -D \cdot s$
'D' here describes the stiffness of the mechanical part like 'ks'. Now it is possible to build a transfer-function.

$$\boxed{G_{s(mech)}(p) = \frac{\delta}{\Delta i} = \frac{k_i}{k_s} \cdot \frac{1}{\left(\frac{m_R}{k_s} \cdot p^2 - 1 \right)}} \quad (2.9)$$

It is obvious to see, that the resulting dynamic system is unstable.

2.2. Inductance

The coil around the stator pole is like a series connection of resistor and inductance with the time-constant 'Tsp' and a gain 'Ksp'. They build an easy PT1 transfer-function (first order delay).

$$T_{Sp} = \frac{L}{R} \text{ and } K_{Sp} = \frac{1}{R}$$

$$\boxed{G_{S(Sp)} = \frac{K_{Sp}}{1 + p \cdot T_{Sp}}} \quad (2.10)$$

2.3. Actuation system

The current converter is the actuator in the bearing system considered. Its dynamic behaviour is so fast, that it is possible to simulate it as a PT1 model. Gain 'KSR' is input voltage to supply voltage and time constant 'TSR' is the half of cycle duration.

$$\boxed{G_{S(SR)} = \frac{K_{SR}}{1 + p \cdot T_{SR}}} \quad (2.11)$$

2.4. Measurement systems

There are two measurement parts in the controlled system, a current sensor and a position sensor. Their time-constants depend on their own cut-off frequency.

$$G_{S((i)mess)} = \frac{K_{(i)mess}}{1 + p \cdot T_{(i)mess}}$$

$$G_{S((\delta)mess)} = \frac{K_{(\delta)mess}}{1 + p \cdot T_{(\delta)mess}} \quad (2.12)$$

2.5. Model block diagram and simulation results

2.5.1. Current control path

The current control path consists of a current converter, coil and current sensor. For the test bearing, the comparison between measurements done and data sheets available demonstrated acceptable parameter conformity.

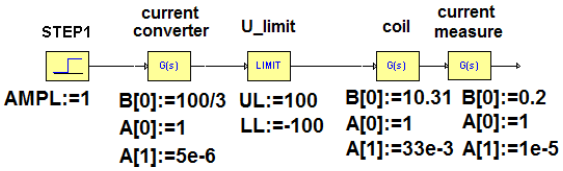

Figure 3 Current-system

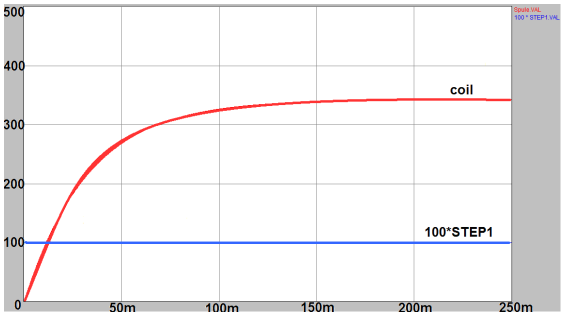

Figure 4 Step response of currentcontrol path

A step with amplitude 1 is applied to the current control path at time t=0. After t=T the function passes the desired value and after t=3*T, current grows up to a final static value. This part of the system needs to be operated with a closed loop current controller.

2.5.2. Mechanical system

The step response of the position controlled system is very important. It is possible to compare the real dynamic behaviour (measured position versus time waveform) with the step response simulated. If the simulated system response looks like the real curve, the mathematical model developed is of sufficient accuracy to determine the compensator parameter. The transient output of the block diagram model representing bearing's mechanical part (without controller) shows figure 5, it's nearly identical to measured data (refer to figure 6).

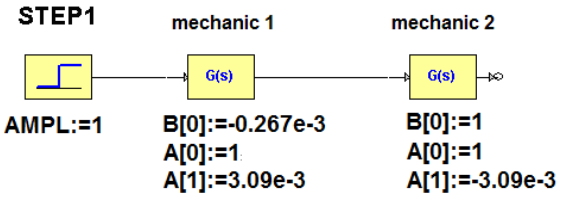

Figure 5 Simulation model of open mechanical system

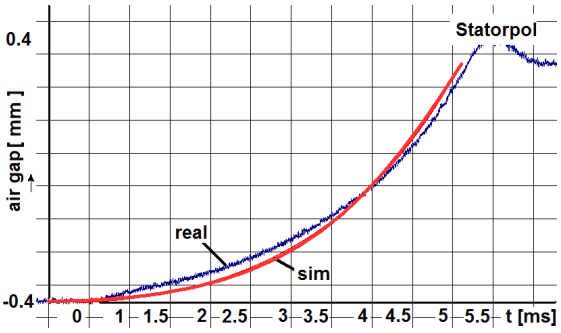

Figure 6 Step response of open mechanical system; Comparison of simulation and measurement

Good to recognize by given illustration above is the monotonous instability; the measured peak at approximately 5.5 sec represents the collision with a mechanical stopper.

3. CONTROLLER CONCEPT

On base of equation (2.9) mechanical system is instable. An additional part – the controller – is needed to control the rotor position. The system contains two "large" time constants 'TSP', 'Tmech'. It offers to use a cascaded controller to achieve the desired control dynamics.

3.1. Current controller

The current controller is the secondary part of a cascaded control loop. Its parmeters can be determined according to the *integral of absolute value of error theorem* (IAE). This guarantees rather swift current transients at only moderate overshoot. The theorem is easy to apply and so it is popular for compensator design in quite different technical fields. The following equations describe the according parameter calculation.

$$G_{R(i)}(p) = K_{P(i)} \cdot \frac{1 + p \cdot T_{1i}}{p \cdot T_{0i}} \qquad (3.1)$$

$$T_{0i} = 2 \cdot \frac{K_{SR} \cdot K_i}{R} \cdot T_{\Sigma i} \qquad (3.2)$$

$$K_i = \frac{U_E}{I_A} \qquad T_{\Sigma i} = T_{SR} + T_{(i)mess} \qquad (3.3)$$

For the test-bearing, current controller parameters are:

$$T_{1i} = \frac{L_{Sp}}{R} = \frac{3{,}2 \cdot 10^{-3} H}{97 \cdot 10^{-3} \Omega} = 33 \cdot 10^{-3} s$$

$$T_{0i} = 2 \cdot \frac{\frac{100V}{3V} \cdot \frac{3V}{15A}}{97 \cdot 10^{-3} \Omega} \cdot \left(5 \cdot 10^{-6} s + 10 \cdot 10^{-6} s\right) = 2{,}06 s$$

$$K_{Sp} = \frac{1}{R} = \frac{1}{97 \cdot 10^{-3} \Omega} = 10{,}31 S$$

Now, the parameters for the closed loop current controller are:

$$K_{P(i)} = \frac{T_{1i}}{T_{0i}} = \frac{33 \cdot 10^{-3} s}{2{,}06 s} = 16 \qquad (3.4)$$

$$K_{I(i)} = \frac{1}{T_{0i}} = \frac{1}{2{,}06 \cdot 10^{-3} s} = 485 s^{-1} \qquad (3.5)$$

3.1.1. Simulation of closed loop current controller

The step response of the closed loop current controller shows, that the desired value was reached in one third of the time compared to the non-controlled (open) system, latter shown in figure 4. After a small overshoot the current follows permanently the setpoint.

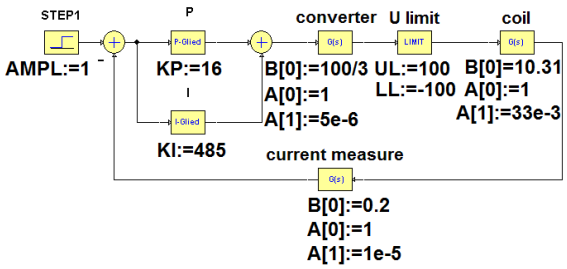

Figure 7 Closed loop current control

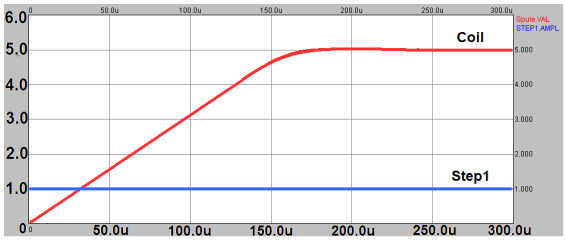

Figure 8 Closed loop current control step response

3.2. Position controller

The most proceedings in optimization are very universal and not well applicable for magnetic bearings. For the position controller it is useful to apply the root locus method after EVANS.

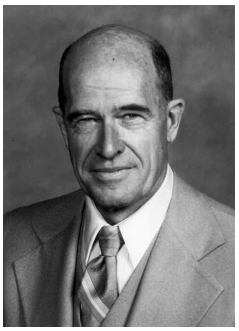

Figure 9 Walter R. Evans (Source: Wikipedia)

With this method it is possible to show, how the roots of the closed loop controlled system depend on the variable (compensator) gain. The approach delivers functions and curves, their shapes can be influenced by adding new pole ore zero roots. The system is only stable when all gain dependent curve locations are on the left side of the complex plane.

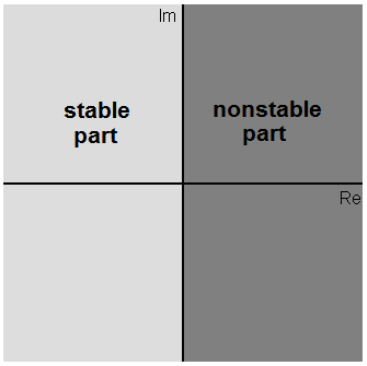

Figure 10 Complex(Gaussian) plane

3.2.1. Model order reduction

It is allowed to disregard the higher orders in the closed loop current controller transfer function. Because only the large time constant is causes the tendency to non stable behaviour of the position controlled system. The replacement allows an easier handling with the position controller design.

$$G_{G(i)} = \frac{b_{0(i)} + b_{1(i)}\,p}{a_{3(i)}\,p^3 + a_{2(i)}\,p^2 + a_{1(i)}\,p + 1} \approx \frac{b_{0(i)}}{a_{1(i)}\,p + 1} \qquad (3.6)$$

Now the position controlled system block structure looks as follows:

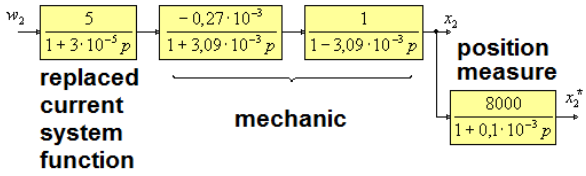

Figure 11 Position controlled system

3.3. Root locus of magnetic bearings

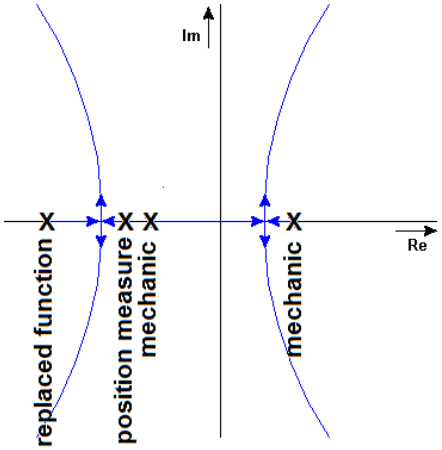

Figure 12 Root-locus P-controller

After closing the controller loop, firstly the roots are situated in the right side of the complex plane. Now it's the aim to modify the curves so, that they travel from the right into the left half plane by adding new poles and/or zeros and adjusting the closed-loop

gain. The pole on the right side of the complex plane can't be compensated because this part of the mathematical structure originates from the given mechanical system. Few differences between reality and model turns the system to become instable. It is only allowed to add poles and zeroes on the left side in the complex plane.

The stable mechanical pole can be overcompensated by two zeroes. A further pole, added in the origin of imaginary and real axes delivers an integral port to the position controller

Because the available energy in the system is limited, the controller's D-Part is considered to be delayed.

$$G_{R(\delta)}(p) = K_{P(\delta)} \cdot \frac{(1+T_{MF} \cdot p)^2}{p} \qquad (3.7)$$

$$G_{R(\delta)}(p) = K_{P(\delta)} \cdot 2 \cdot T_{MF} \cdot \left(1 + \frac{1}{2 \cdot T_{MF} \cdot p} + \frac{T_{MF}}{2} \cdot p\right)$$

$$\frac{T_V}{T_1} = 3...50 \quad [1][2]$$

$$G_{R(\delta)}(p) = K_{R(\delta)} \cdot \left(1 + \frac{1}{T_N \cdot p} + \frac{T_V \cdot p}{(1+T_1 \cdot p)}\right) \qquad (3.8)$$

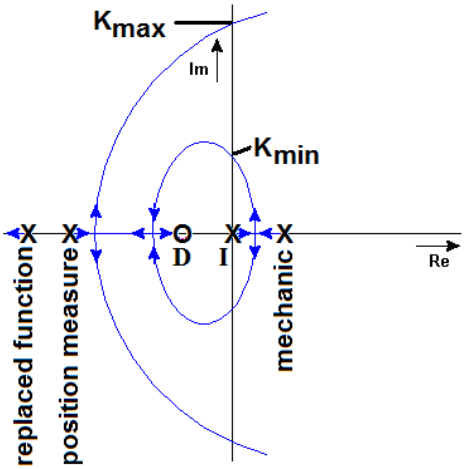

Figure 13 PID-controlled position loop

3.4. Stability analysis

The root-locus shows, that the PID controlled system is stable in an operational range between Kmin to Kmax. These limits can be determined by using the ROUTH-scheme. For the test bearing limits are calculated as follows.

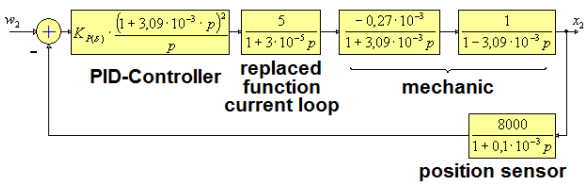

Figure 14 Closed position control-loop

$$G_{O(\delta)}(p) = \frac{-10{,}68 - 33 \cdot 10^{-3} p}{-9{,}27 \cdot 10^{-12} \cdot p^4 - 3{,}99 \cdot 10^{-7} \cdot p^3 - 3 \cdot 10^{-3} \cdot p^2 + p}$$

$$G_{G(\delta)}(p) = \frac{G_{O(\delta)}(p)}{1 + G_{O(\delta)}(p)} \qquad (3.9)$$

$$G_{O(\delta)}(p) = \frac{K_{P(\delta)} \cdot (p + 323{,}63)}{2{,}81 \cdot 10^{-10} \cdot p^4 + 1{,}21 \cdot 10^{-5} \cdot p^3 + 89{,}7 \cdot 10^{-3} \cdot p^2 + \left(K_{P(\delta)} - 30{,}3\right) \cdot p + 323{,}63 \cdot K_{P(\delta)}}$$

4	$2{,}81 \cdot 10^{-10}$	$89{,}7 \cdot 10^{-3}$	$323 \cdot K_{P(\delta)}$	**zeros**
3	$1{,}21 \cdot 10^{-5}$	$\left(K_{P(\delta)} - 30{,}3\right)$	0	
2	$-23 \cdot 10^{-6} \cdot \left(K_{P(\delta)} - 3887{,}82\right)$	$323 \cdot K_{P(\delta)}$	0	3887,82
1	$\frac{K_{P(\delta)}^{\ 2} - 3750 \cdot K_{P(\delta)} + 117810}{K_{P(\delta)} - 3887{,}82}$	0	0	3718,31 31,68
0	$323 \cdot K_{P(\delta)}$	0	0	

Figure 15 ROUTH scheme for tes -bearing

The zeros in the rows show the limits of gain. Now compensator function can be writeen in the following form

$$G_{R(\delta)}(p) = (31{,}7...3718) \cdot \left(1 + \frac{1}{6{,}18 \cdot 10^{-3} \cdot p} + \frac{1{,}55 \cdot 10^{-3}}{(1 + 31 \cdot 10^{-6} \cdot p)} \cdot p\right)$$

3.4.1. Disturbances and limits

Before starting simulation, in reality there are some disturbances we can't ignore. Noise and disturbance forces appear to the system. The measured position signal must be filtered at the input of the PID-controller. Another influence is the changing inductance because of the varying air gap.

$$U_{Sp} = R_{Sp} \cdot i(t) + L \cdot \frac{di(t)}{dt} + k_i \cdot \frac{d\delta(t)}{dt} \qquad (3.10)$$

$$R_{mag} \approx \frac{\delta}{\mu_0 \cdot A_{Fe}} \qquad L = \frac{N^2 \cdot \mu_0 \cdot A_{Fe}}{\delta} \qquad (3.11)$$

$$L \sim \frac{1}{R_{mag1}} \qquad L \sim \frac{1}{R_{mag2}} \qquad (3.12)$$

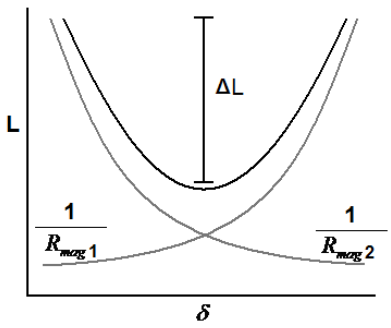

Figure 16 Example of inductance variation a s a function of the air gap

Last but not least, mechanical and electrical limits are:

- Limited input voltage of current converter
- Limited voltage source of current converter
- Limited output current of current converter
- A mechanical bearing limits the air gap

Because of these limits, the system can't react on harsh input signal changes (like steps). So a desired value filter reduces the energy to lift of the shaft.

3.5. Simulation of the closed loop position system

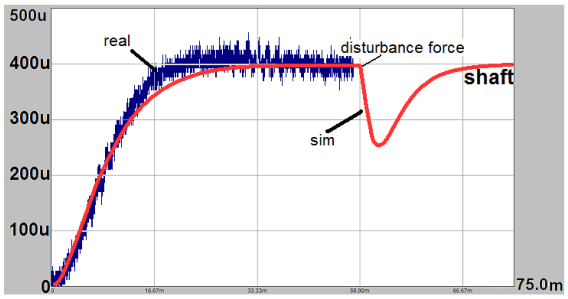

Figure 17 Desired value functions

The picture shows the lift-of of the shaft. The blue coloured wave form represents the real answer of test bearing; the red curve is the simulated system response.

The position changes with PT2-shaped (delayed) desired value. In simulation additionally a load operation (disturbance force) is applied at 50 msecs. The controller handles the disturbances well and puts the shaft back to desired value.

4. BEHAVIOUR OF THE CLOSED LOOP

For an well adjusted controller there are two criterions to fulfill: Command action as well as disturbance reaction of the control loop.
The elongation of the rotor increases with more disturbance force. To reduce this over- and undershoot, gain must be raised. A shorter transient time of movement is reached by high gain, too.

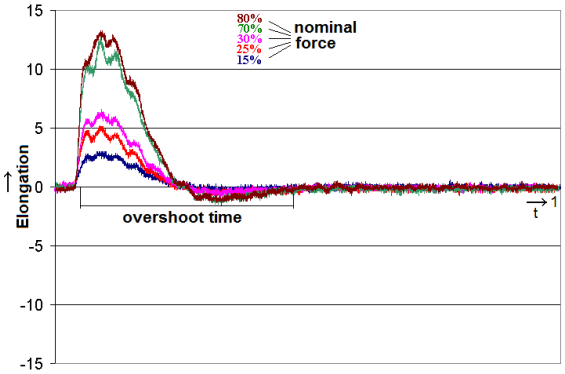

Figure 18 Elongation to nominal force

4.1. Setpoint forming/filtering

With a suitable PT2-filter additionally applied to the desired value branch, the overshoot can be reduced.

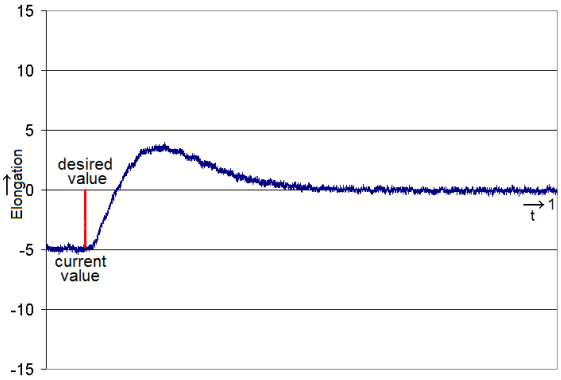

Figure 19 Overshoot time and des.-val.-filter

4.2. Resume

The optimal controller gain values are between a system damping coefficient from 0.7 to 1. Then the system then only tends to moderate oscillations. To reduce the influence of disturbance forces, gain should be near the most left branching point in the root-locus.

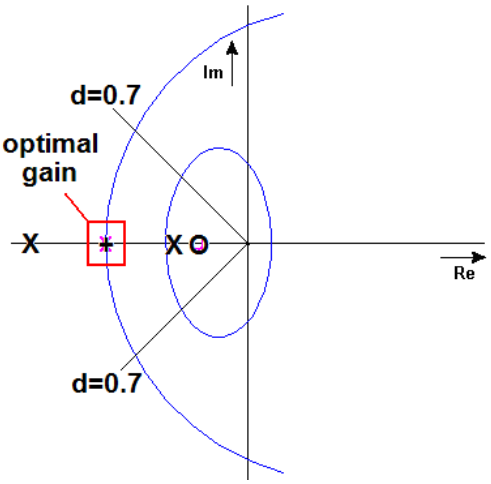

Figure 20 Optimal gain, damping=1

4.3. Fuzziness in pole compensation

There are always differences between simulation model and reality. Zeros of the PID-Controller can miss the mechanical pole (no full pole compensation). Following pictures show that the system is stable, anyway, i.e. the controller developed is robust enough to ensure a good system dynamic also in case of plant parameter variances

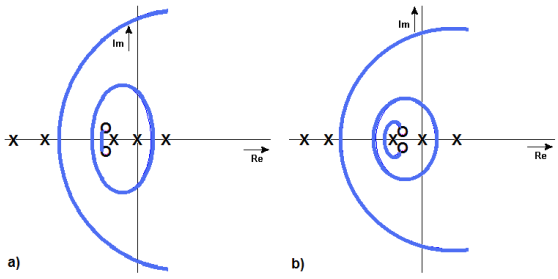

Figure 21 System robustness in case system parameter variations (no exact pole compensation)

4.4. System requirements

Not every root-locus gives a stable or even an optimal result. Then certain system parameters need to be modified. Such parameters in the current controlled loop are:

- Supply voltage of current converter
- Inductance of bearing coils
- Pulse frequency
- Current measurement system (cut off frequency)

Further parameters can be changed in the position controlled system:

- Air gap
- Rotor mass
- Position measurement system (cut off frequency)

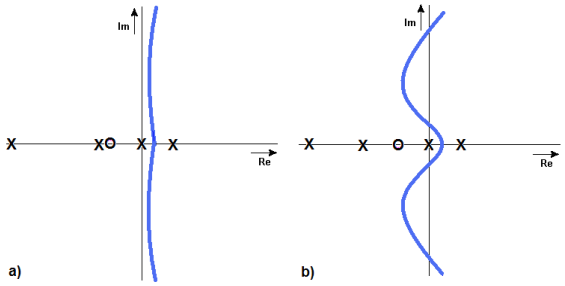

Figure 22 Samples for faulty pole/zero arrangements, system parameters to be improved.

5. DIGITAL CONTROLLER

To use programmable integrated circuits like state-of-the-art microcontrollers or FPGA's makes it easy to implement the mathematical PID-controller-formulas on a chip. One significant advantage is the exact adjustment of parameters without any drifting by temperature or electro-magnetic influences.

The Analogue-Digital-converter digitalizes the analogue signal in n-quantized steps. By a constant sampling frequency, at every (equidistant) sampling point the controller gets a new A-D-value. This process must be described by mathematical formulas.

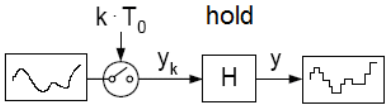

Figure 23 Sample and hold

5.1. z-Transformation and digital controller

For I-Part of the digital controller in this context it is fully sufficient to use the TUSTIN approximation:

$$F(p)=\sum_{k=0}^{\infty} f(k\cdot T_0)\cdot e^{-k\cdot T_0\cdot p} \quad \text{k=1, 2, 3…} \qquad (5.1)$$

$$e^{T_0\cdot p}=z \qquad p=\frac{1}{T}\cdot\ln(z) \qquad (5.2)$$

$$p=\frac{1}{T_0}\cdot 2\cdot\left[\frac{z-1}{z+1}+\frac{1}{3}\cdot\left(\frac{z-1}{z+1}\right)^3+\frac{1}{5}\left(\frac{z-1}{z+1}\right)^5+\ldots\right] \qquad (5.3)$$

Equation (5.3) reduced to first order leads to the TUSTIN formula:

$$\boxed{p=\frac{2}{T_0}\cdot\left[\frac{z-1}{z+1}\right]} \qquad (5.4)$$

For the D-part of the digital controller it's possible to use following equation:

$$y_k=y_{(k-1)}+T_0\cdot u(k) \;\rightarrow\; y_z\cdot\left(1-z^{-1}\right)=T_0\cdot U(z)$$

$$y_z=\frac{T_0\cdot z}{1-z}\cdot U(z) \qquad (5.5)$$

$$\frac{1}{p}\rightarrow \qquad \boxed{p\approx\frac{z-1}{T_0\cdot z}} \qquad (5.6)$$

After these approximations the z-transformed terms are set into the analogue controller formula. After some mathematical conversions the general digital transfer function is:

$$G_R(z)=\frac{d_0+d_1z^{-1}+d_2z^{-2}}{1+(c_1-1)z^{-1}-c_1z^{-2}} \qquad (5.7)$$

$$d_0=C_V\cdot\left[1+\frac{T_0+T_1}{2T_N}+\frac{T_V+T_1}{T_0}\right]$$

$$d_1=C_V\cdot\left[-1+\frac{T_0}{2T_N}-\frac{2(T_V+T_1)}{T_0}\right]$$

$$d_2=C_V\cdot\left[\frac{T_V+T_1}{T_0}-\frac{T_1}{2T_N}\right]$$

$$c_1=-\frac{T_1}{T_0+T_1} \qquad C_V=\frac{K_{R(\delta)}}{1+\frac{T_1}{T_0}}$$

The immediate on-chip controller implementation requires the according difference equation:

$$U(k) = d_0 \cdot e_k + d_1 \cdot e_{(k-1)} + d_2 \cdot e_{(k-2)} + (1 - c_1) \cdot U_{(k-1)} + (1 - c_1) \cdot U_{(k-2)}$$

The PI current controller looks like (5.7). Only the D-part must be zero. The digital controller simulation displays nearly the same results like in analogue simulation.

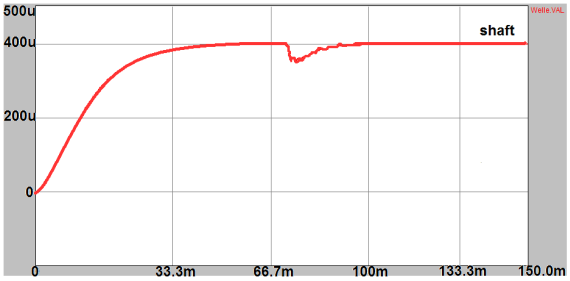

Figure 24 Digital controlled system answer

6. CONCLUSIONS

As illustrated above, a systematic, mathematical based and simulation aided controller synthesis, even for such a highly non-linear and instable process “magnetic bearing” could be performed successfully. It’s easy to see, what an important and powerful tool simulation could be. This technology –if applied competently- is able to provide early forecasts of static and dynamic behaviour already for systems and components still not exist in hardware.

Further investigations will target to the application of structure optimum high gain controller algorithms. In addition to several state-space approaches already wide spread, this could be different predictive or special robust control philosophies like “Principle of Localization”.

7. LITERATURE

[1] Ringo Lehmann, “Regelung magnetischer Lager” Westsaxon University of Applied Sciences, pp. 9, 2008.

[2] Lehrbriefe Proske, Regelungstechnik I und II

[3] Heinz Unbehauen, Regelungstechnik I: Klassische Verfahren zur Analyse und Synthese linearer kontinuierlicher Regelsysteme, Fuzzy-Regelsysteme, 10.Auflage, Vieweg Verlag